Environment International 141 (2020) 105727

Contents lists available at ScienceDirect

Environment International

journal homepage: www.elsevier.com/locate/envint

Shale gas development in China: Implications for indoor and outdoor air quality and greenhouse gas emissions

Yanxu Zhang[a,*], Haikun Wang[a], Yun Han[a,1], Danhan Wang[a,2], Ge Zhu[b], Xi Lu[c,d]

[a] Joint International Research Laboratory of Atmospheric and Earth System Sciences, School of Atmospheric Sciences, Nanjing University, Nanjing 210023, PR China
[b] State Key Laboratory of Pollution Control and Resource Reuse, School of Environment, Nanjing University, Nanjing 210023, PR China
[c] School of Environment and State Key Joint Laboratory of Environment Simulation and Pollution Control, Tsinghua University, Beijing 100084, PR China
[d] State Environmental Protection Key Laboratory of Sources and Control of Air Pollution Complex, Beijing 100084, PR China

ARTICLE INFO

Handling Editor: Yong-Guan Zhu

ABSTRACT

Holding the largest recoverable reserves over the world, China makes an ambitious plan to increase shale gas production. Here we use an integrated approach to quantify its impact on indoor and outdoor air quality and greenhouse gas emissions. This approach includes emission estimation, three-dimensional atmospheric chemistry modeling, and human health assessment. Although the production of shale gas generates $PM_{2.5}$, this risk is outweighed by the benefits of the decreased $PM_{2.5}$ resulted from coal combustion when shale gas replaces coal as a fuel source. The total avoided premature deaths are 14,000 (10,650–17,160 as 95% confidence interval) and 13,400 (10,350–17,100) in 2017, resulted from the outdoor and indoor pathways, respectively. Future scenario analysis suggests deploying shale gas in the residential sector, but the greenhouse gas emission reductions are minimal if replacing biomass fuel. In production regions, a net deterioration of air quality is predicted if deploying shale gas in the power and industrial sectors, but a net benefit is calculated if deploying in the residential sector. Our study calls for more stringent emission control during upstream processes, and comprehensive consideration of the cost and benefits in both the production and consumption regions.

1. Introduction

Natural gas is a much cleaner energy source than other fossil fuels such as coal and oil for the emission intensity (emission per unit energy generated) of major air pollutants (e.g. SO_2 and PM) in the combustion process (IIASA, 2019). The production of natural gas from shale is enabled by horizontal drilling and hydraulic fracturing techniques, and the rapid growth of its production started in the US in 2007–2009 (Howarth et al., 2011; US, 2019a). By replacing other fossil fuels (mainly coal), it reduces air pollutant emissions such as CO_2, NOx, SO_2, $PM_{2.5}$ and Hg from power plants in the US (de Gouw et al., 2014; Zhang et al., 2016). Even though the net environmental effect remains controversial (Howarth et al., 2011; Guo et al., 2016), the success of the US in exploiting shale gas has stimulated many other countries, including China, to exploit their shale gas resources (Krupnick et al., 2014).

China has the largest technically recoverable reserves of shale gas in the world at 31.6 trillion cubic meters (tcm) (US, 2019b). Shale gas development is heavily promoted by China and the production has increased drastically in the past five years as a result of governmental subsidization, improving infrastructure, and advancing technologies (Guo et al., 2016; US, 2020). The total production increased from 0.15 billion cubic meters (bcm = 10^9 m^3) in 2013 to 9.03 bcm in 2017 with an annual mean increase rate of 278%[10]. Based on the plan of the National Energy Administration of China (NEAC) made in 2016, the production will achieve 30 bcm in 2020 and 100 bcm in 2030 (NEAC, 2020).

Similar to the US, the fast increase in shale gas production is expected to alleviate the heavy outdoor air pollution in China. Previous works have shown that replacing coal with shale gas resulted in a 62.8–75.5% decrease in monthly observed $PM_{2.5}$ concentration in a case study (Song et al., 2015). Increased coal-based synthetic natural gas production would result in a up to 20% decrease of $PM_{2.5}$ concentrations in the Beijing-Tianjin-Hebei region in 2020 (Qin et al., 2017). Besides, shale gas is expected to replace coal and biomass fuel use for cooking and heating in the residential sector that occurs in an indoor environment, which could reduce indoor PM concentrations.

* Corresponding author.
E-mail address: zhangyx@nju.edu.cn (Y. Zhang).
[1] Department of Biostatistics, UCLA School of Public Health, Los Angeles, CA 90095, USA.
[2] College of Environmental Science and Forestry, State University of New York, Syracuse, NY 13210, USA.

https://doi.org/10.1016/j.envint.2020.105727
Received 18 January 2020; Received in revised form 5 April 2020; Accepted 6 April 2020

Indeed, the average indoor PM concentrations in families using non-solid fuels (including natural gas) were found about half of the level in homes burning solid fuels (such as coal and wood) (Du et al., 2018). This replacement thus has health benefits to the Chinese population because indoor emissions from in-home coal and wood combustion are carcinogenic (group 1) and probable carcinogenic (group 2A) to humans, respectively (Dean Hosgood et al., 2010).

On the other hand, substantial air pollutants and greenhouse gases (GHG) emissions (in the form of methane leakage or vented with or without flaring) are associated with upstream processes of shale gas (production, processing, transmission, and distribution) (Qin et al., 2017; Chang et al., 2014). This emission could deteriorate local air quality and cause global warming that may offset the benefits resulted from fuel substitution by shale gas. Previous studies have focused on the effects of outdoor air quality and GHG emissions associated with the shale gas industry under assumed production scenarios (Qin et al., 2017; Qin et al., 2018), with many of the other impacts remained unquantified. The objectives of this study are thus to evaluate: (1) the impact of shale gas consumption on indoor air quality; (2) outdoor air quality impact at shale gas production regions; and (3) the air quality impacts and GHG emissions associated with actual shale gas production and future scenarios.

2. Methodology

We use an integrated assessment tool to calculate the changes in air quality and GHG emissions resulting from the upstream processes of shale gas and its replacement for the combustion of other fuels. This tool integrates shale gas activity allocation, air pollutants emission estimate, air quality modeling, and health impact evaluation (Fig. 1).

2.1. Shale gas activity

We use the shale gas production data from a national market survey in 2017 as the current state (HBERC, 2018) and the projection of NEAC as an outlook for 2030 (NEAC, 2020). The national total shale gas production in 2017 is 9.03 bcm from Sichuan, Chongqing, and Yunnan Provinces in Southwest China (HBERC, 2018). Limited by gas pipeline infrastructure, the consumption of the harvested gas is mainly confined in nearby provinces: 40.2% consumed locally by Southwest China and 45.8% by Central China (Henan, Hubei, and Hunan provinces). East China consumes 9.8% and other regions in total consume the remaining 4.3% (Fig. S1A). The consumption data for different regions (Southwest, East, Central, and other parts of China) are distributed to each province based on population. This results in that Sichuan and Henan Provinces consumed the most shale gas in 2017 (1.5 and 1.7 bcm, respectively), followed by Hunan (1.3 bcm) and Hubei (1.1 bcm) provinces. Other provinces in Central and Southwest regions, including Yunnan (0.87 bcm), Guizhou (0.65 bcm), and Chongqing (0.55 bcm) had fewer consumptions. In 2017, the consumption of shale gas mainly occurred in the residential (including both residential and commercial cooking and heating, 74%) and industrial (26%) sectors (HBERC, 2018).

Based on the plan of NEAC (NEAC, 2020), the annual production of shale gas will achieve 100 bcm in 2030, and the production regions remain in Sichuan and nearby regions. We assume the consumption distribute following the provincial primary energy consumption in 2030 (IIASA, 2019). This is a reasonable assumption due to the political willingness to expand pipeline infrastructure by the Chinese central government, and many large-scale natural gas pipeline expansion projects are built or planned, e.g. the ones from Sichuan to East China and Xinjiang Synthetic Nature Gas Pipeline Project (NDRC, 2019). Some of the provincial and lower-level governments are subsidizing the construction of local pipelines, especially last-meter distribution pipelines for rural areas with less population density (Mao et al., 2005). Incentives are also offered to build gas liquefaction or compression plants near shale gas zones, which facilitates shale gas shipment beyond the reach of pipeline network (NEAC, 2019). The resulted distribution of shale gas consumption in 2030 is the highest over Shandong (8.3 bcm), Guangdong (8.1 bcm), and Jiangsu (7.7 bcm) provinces, followed by Henan (6.8 bcm), Hebei (6.4 bcm), and Zhejiang (5.3 bcm) provinces (Fig. S1B).

2.2. Emission

Significant amount of air pollutants and GHGs (SO_2, NOx, VOC, $PM_{2.5}$, PM_{10}, BC, OC, CO_2, and CH_4) are emitted during the shale gas production process, including pad preparation, well drilling, well cementation, fracturing, and completion. The emissions (E_{pro}) are calculated based on the number of shale gas wells (N_{well}) and emission factors per well (EF_{well}):

$$E_{pro} = N_{well} \times EF_{well} \quad (1)$$

As no official statistical data is available, N_{well} is estimated based on the total shale gas production and the average per-well production rate (HBERC, 2018), while EF_{well} is collected from the literature (Tables S1 and S2). The middle-range values are adopted as the best estimate, whereas the low- and high-range EF_{well} are used to estimate its uncertainty range. The upstream GHG emissions (E_{up}) are calculated based on total shale gas production and its lifecycle carbon intensity (Qin et al., 2017). Different GHG emissions (CH_4 and CO_2) are compared using equivalent CO_2 emissions (CO_{2eq}) based on its GWP values over 100-year (GWP_{100}) and 20-year (GWP_{20}) time horizons. The same mass of CH_4 traps 28 times more heat than CO_2 over a 100 year time horizon, and 84 times more in a 20 year horizon (Myhre et al., 2013).

The reductions of major air pollutants and GHG emissions during fuel combustion resulted from substituting shale gas for other fuels such as coal and biomass fuels are considered. The Greenhouse Gas – Air Pollution Interactions and Synergies (GAINS) model is employed in this study as the base case emission inventories of air pollutants in 2017 and

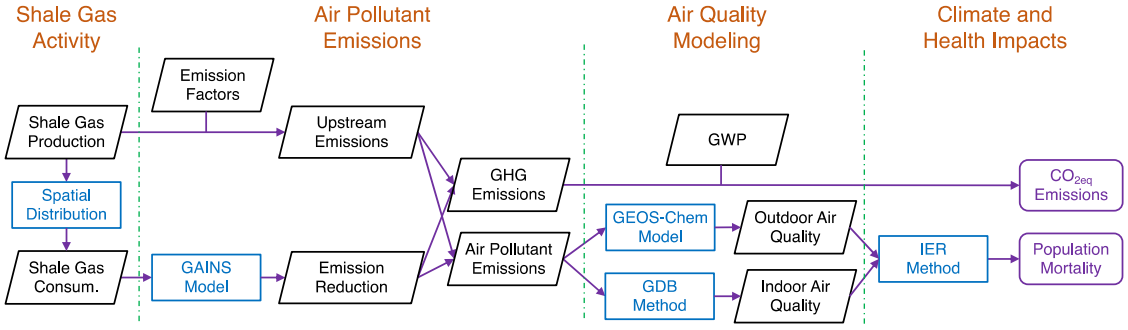

Fig. 1. Methodology framework for analyzing the GHG emissions and health effects of shale gas development. GAINS, GWP, GDB, and IER stand for the Greenhouse Gas-Air Pollution Interactions and Synergies model, global warming potential, global disease burden, and integrated exposure-response model, respectively.

2030 (IIASA, 2019). The model calculates the historical and future emissions of air pollutants and GHG for different provinces of China (Amann et al., 2008). We use the results of the ECLIPSE_V5a_CLE scenario that provides air pollutant and GHG emission factors for different sectors and sources at a provincial level during 1990–2030 (Amann et al., 2008). The mass of substituted fuels by shale gas (m) is calculated based on heat values and efficiency of different fuels:

$$m_{fuel} \times H_{fuel} \times \eta_{fuel} = m_{gas} \times H_{gas} \times \eta_{gas} \quad (2)$$

where H and η are the heat values and energy efficiencies of fuels ($fuel$ = coal or biomass fuels; gas = shale gas) (Table S3 and S4). The replaced emissions by shale gas (E_{sub}) are calculated by multiplying the substituted fuel mass (m_{fuel}) and the corresponding emission factors (EF_{fuel}, Table S5-7):

$$E_{sub} = m_{fuel} \times EF_{fuel} \quad (3)$$

The uncertainty range of E_{sub} is estimated based on the variability of EF_{fuel} given by the GAINS model.

2.3. Air quality modeling

We use the GEOS-Chem model (version v11-01) to simulate air pollutant concentrations (www.geos-chem.org) (Zhang et al., 2015). The model is driven by assimilated meteorological data archived from the Goddard Earth Observing System (GEOS) general circulation model. It includes 47 vertical levels extending up to the mesosphere. The model is configured as a nested-grid system with the coarse grid covering the globe at a horizontal resolution of 4° × 5° and the fine grid covering East Asia at 0.25° × 0.3125° (~25 km). The model contains a gas phase HOx–NOx–VOC-ozone-BrOx chemistry (Miller et al., 2017), and a detailed sulfate-nitrate-ammonium-carbonaceous-dust-sea salt aerosol chemistry, which is coupled to gas phase chemistry (Fisher et al., 2016). Natural sources, including biogenic emissions (MEGAN) (Guenther et al., 2012) and biomass burning (GFED4) (Randerson et al., 2018) are also included.

Three model scenarios are calculated for 2017: (i) a base case scenario with 2010 Multi-Resolution Emission Inventory for China (MEIC) emission inventory scaled to GAINS 2015 level; ii) a shale gas inventory with additional emissions from coal combustion that had been replaced by shale gas; and iii) production scenario with additional emissions from shale gas production. There are seven scenarios for 2030: (i) a base case scenario is conducted with anthropogenic emissions scaled to GAINS 2030 level; and four additional shale scenarios with the substituted emissions subtracted from the base case scenario. In these scenarios, shale gas is exclusively allocated to replace coal use in the (ii) Residential, (iii) Industrial, and (iv) Power sectors in turn. An additional scenario (v, Sector2017) assumes the same sector distribution for shale gas consumption in 2030 as 2017. The sixth scenario (vi, Biomass) assumes shale gas is substituting for biomass fuel combustion. The last scenario considers the additional emissions from shale gas production. The $\Delta PM_{2.5}$ concentrations are calculated as the differences between the shale scenarios and the base cases in the corresponding years (Table 1).

The air pollutant emissions from shale gas production are assigned to model grids located at major shale gas production areas in southwest China. The provincial-level emission reductions from shale gas substitution are distributed to GEOS-Chem model grids following the spatial and temporal pattern of the MEIC inventory in 2010 (Center for Earth System Science of Tsinghua University, 2019).

The improvement of indoor air quality from switching from solid to non-solid fuels depends on many factors such as fuel types (coal or wood), seasons (winter or other seasons), and room functions (kitchen or bedroom) (Du et al., 2018). Due to the lack of data, we use average $PM_{2.5}$ concentrations for families with solid or non-solid fuels following the WHO Global Disease Burden (GDB) study (World Health Organization, 2019).

2.4. Health impact of outdoor air quality

We consider only $PM_{2.5}$ in this study as it dominates the health impact of air pollution in China (Matus et al., 2012), and other pollutants can be included similarly. The premature mortality (M) associated with long-term ambient $PM_{2.5}$ exposure for both adults and children are evaluated. The detailed method is described in Wang et al. (Wang et al., 2017). Briefly, the associated premature death from four major causes of mortality, i.e. ischemic heart disease (IHD), chronic obstructively pulmonary disease (COPD), cerebrovascular disease (stroke), and lung cancer (LC) are quantified according to the global burden of disease project (Stanaway et al., 2018) with an integrated exposure-response (IER) model (Burnett et al., 2014). The IER model quantitatively describes the concentration-response relationship for ambient $PM_{2.5}$ concentrations by integrating data from cohort studies of ambient air pollution, indoor burning of solid fuels, and active and secondhand smoking. The changes in mortality (i.e. avoided deaths or excess deaths) are calculated as the difference between the base cases and the shale gas scenarios:

$$M = AF \times B \times P \quad (4)$$

$$AF = \frac{\sum p_i (RR_i(C_i) - 1)}{\sum p_i RR_i(C_i)} \quad (5)$$

where AF is the attributable fraction of $PM_{2.5}$ pollution; B is the incidence rate of deaths due to specific disease; and P is the exposed population (taken as the total population). The subscript i means individual grid cell. RR is the relative risk calculated based on the integrated exposure-response functions developed by Burnett et al. (Burnett et al., 2014):

$$RR(C) = \begin{cases} 1 + \alpha[1 - exp(-\gamma(C - C_0)^{\delta})] for C > C_0 \\ 1 for C \le C_0 \end{cases} \quad (6)$$

Table 1
Emission scenarios simulated by the GEOS-Chem model.

Scenario	Sector	Fuel	Description
2017			
i. Base			GAINS 2015 emission inventory
ii. Shale	Residential and industrial sectors	coal	74% of shale gas consumption in the residential/commercial sectors, and 26% in the industrial sector.
iii. Production			Additional emissions from shale gas production
2030			
i. Base			GAINS 2030 emission inventory
ii. Residential	Residential	coal	All shale gas used in the residential sector
iii. Industrial	Industrial	coal	All shale gas used in the industrial sector
iv. Power	Power	coal	All shale gas used in the power sector
v. Sector2017	Residential, industrial, and power sectors	coal	Shale gas used in multiple sectors with fractions in each sector as the same as that in 2017.
vi. Biofuel	Residential	biofuel	All shale gas used in the residential sector
vii. Production			Additional emissions from shale gas production

where C is the $PM_{2.5}$ concentration; C_0 is the counterfactual concentration below which there is no additional risk; and α, γ, and δ are parameters for the exposure-response curve. We use the range in these three parameters to calculate the uncertainty of RR for $PM_{2.5}$ exposure (Wang et al., 2017). Monte Carlo simulations are conducted for 1000 sets of randomly generated C_0; α, γ, and δ values for each health endpoint, and the 95% confidence intervals (CI95) are used to bracket uncertainty with the median value as the best estimate.

2.5. Health impact of indoor air quality

We use the population mainly relying on solid fuel (including coal and biomass, denoted as P_{SF}) as a proxy indicator to estimate the health impact associated with indoor air quality from shale gas substitution following the WHO GDB study, which assesses mortality and disability from major diseases, injuries, and risk factors (World Health Organization, 2019). The reduction in the P_{SF} (ΔP_{SF}) is estimated based on the total shale gas consumption (m_{gas}) in the residential sector, the heat value of natural gas (H_{gas}), and the per-capita residential energy needs (E_{res}) (NBSC, 2016):

$$\Delta P_{SF} = \frac{m_{gas} \times H_{gas}}{E_{res}} \quad (7)$$

The calculated ΔP_{SF} is 22 million in 2017 and is projected to 330 million in 2030. The avoided deaths associated with switching from solid fuel to shale gas resulted from indoor air pollution (ΔM) is estimated proportional to the resulted ΔP_{SF}:

$$\frac{\Delta M}{M_{baseline}} = \frac{\Delta P_{SF}}{P_{SF}} \quad (8)$$

The baseline estimate ($M_{baseline}$) and its CI95 ranges for the death caused by indoor air pollution from solid fuels for China in 2017 are from the Institute for Health Metrics and Evaluation (https://vizhub.healthdata.org), and the P_{SF} is from Yu et al. (2018). The same $M_{baseline}$ and P_{SF} are applied to 2030 due to the lack of proper projections. The calculated ΔM is a net effect of energy switching, i.e. the difference between the mortality with solid and non-solid fuels.

3. Results and discussion

3.1. Changes in emissions

Fig. 2A shows the emission changes due to shale gas substitution in 2017. The reduced emissions are 393, 62, 123, 148, 62, 42, and 65 kt/yr (kilo tonnes per year) for SO_2, NOx, PM, VOC, BC, and OC, respectively. This emission reduction accounts for 0.29–4.8% of the national total in 2017, but the percentage decreases are much larger over the provinces with high shale gas consumption. For instance, the SO_2 emission decreased by 9.2%, 5.3%, 3.6%, and 2.6% in Sichuan, Hunan, Hubei, and Henan Province, respectively. The reduction in GWP_{100} and GWP_{20} emissions are 106 and 138 Mt/yr, respectively. The decreased emissions are mainly from the residential sector for these pollutants and GWPs (Fig. 2A), especially for PM, VOC, BC, and OC because of the relatively higher emission factors in this sector. For SO_2 and NOx, however, the industrial sector plays a larger role by contributing 15% and 35%, respectively.

Fig. 2B shows the projected emission reduction due to shale gas substitution in 2030. Depending on the sectors and fuel types that shale gas is replacing, the reduction in emission varies drastically. Taking SO_2 as an example, the emission reduction is only 375 kt/yr if all the coal substitution happens in the power sector, 727 kt/yr in the industrial sector, but up to 4059 kt/yr in the residential sector. This is primarily because the power sector has the most stringent emission controls among these sectors, whereas generally uncontrolled in the residential sector. The industrial sector lies in between with a large fraction of low-emitting coal boilers, especially for SO_2 and PM. The Biomass scenario has only 413 kt/yr in SO_2 emission reduction, largely because of the lower sulfur content in biomass fuels than coal, but its reduction in $PM_{2.5}$ (2500 kt/yr) is even larger than the residential sector (1840 kt/yr). The emissions vary for 2–3 orders of magnitudes for BC (1.2–664 kt/yr) and OC emissions (1.8–1040 kt/yr) across different scenarios. Besides emission control devices, the residential sector has generally lower combustion temperature and poorer ventilation than the industrial and power sectors, which results in more BC and OC emissions due to incomplete combustion (Chen et al., 2009). This is consistent with previous studies regarding synthetic natural gas and residential emissions (Qin et al., 2017; Liu et al., 2016).

The reduction in GWP_{100} and GWP_{20} for different shale gas substitution scenarios also varies significantly (Fig. 2B). For example, Residential and Power scenarios have relatively larger GWP_{20} (1900 and 1600 Mt/yr, respectively) than the Industrial scenario (530 Mt/yr). The Biomass scenario, however, has the lowest GWP emission reductions (190 Mt/yr as of GWP_{20}) after shale gas substitution as the GWP emissions from biomass burning are close to that of shale gas (IIASA, 2019).

Shale gas will likely be consumed in more than one sector in 2030. If assuming the sector allocation keeps the same as that in 2017 (Sector2017), it results in emission reductions of 3075 kt/yr, 535 kt/yr, 1318 kt/yr, 1586 kt/yr, 660 kt/yr, 471 kt/yr, 734 kt/yr, 1200 Mt/yr, and 1600 Mt/yr for SO_2, NOx, $PM_{2.5}$, PM_{10}, VOC, BC, OC, GWP_{100}, and GWP_{20} respectively (Fig. 2B). This accounts for only ~3% of projected national total NOx and VOC emissions in 2030, which are mainly contributed by the industrial and transportation sectors that have little shale gas substitution. The fractions are higher (12–16%) for SO_2 and PM owing to higher contributions from the residential sector. The highest fractions (~47%) are for BC and OC, as the residential sector is the dominant source of these pollutants. For GWP_{100} and GWP_{20}, the fractions are 7.7% and 8.3%, respectively.

We contrast the excess emissions during upstream processes with the emission reduction from fuel substitution (Fig. 2). In 2017, the excess air pollutant emission mainly consists of NOx and VOC (17 kt/yr and 4.2 kt/yr, respectively), while other pollutants are smaller or close to 1 kt/yr (Fig. 2A). These pollutants are mainly from operational energy use by on-site equipment during well drilling and hydraulic fracturing processes (Chang et al., 2014). The GWP_{100} and GWP_{20} emissions from upstream processes are 14 and 24 Mt/yr, respectively. In 2030, the NOx and VOC emissions are projected to amount to 190 kt/yr and 47 kt/yr, respectively. The GWP_{100} and GWP_{20} emissions from upstream processes range 160–200 Mt/yr and 220–350 Mt/yr, respectively. Compared with the air pollutant emission reduction associated with fuel substitution, the excess emissions from upstream processes are much smaller except NOx, however, these emissions are more concentrated in shale producing regions in Sichuan and nearby regions. For GWP, the emission reductions from shale gas substitution are much larger than that from upstream processes, except for the Biomass scenario, which has similar GWP emissions as coal (Fig. 2B).

The average or marginal air pollutant emission reduction by unit volume of shale gas replacement decreases continuously due to more stringent emission controls for the other fuels (Fig. 3). For instance, the average SO_2 and NOx emissions decrease by 29% and 22%, respectively, from 2017 (44 and 6.9 kt/bcm) to 2030 (31 and 5.4 kg/bcm, assuming the sector allocation in 2030 keeps the same as that in 2017, i.e. Sector2017 scenario). The decreases for other pollutants, such as $PM_{2.5}$ and BC are smaller or not changed because the major contributors of these pollutants are the residential sector, which undergoes nearly no emission control regulations (Shen et al., 2019). The changes in GWP are also negligible as the GAINS model assumes nearly constant carbon intensity for coal combustion during 1990–2030 (IIASA, 2019). This might be true because of the low participation rates and policy challenges of carbon capture technology in China (Jiang et al., 2020). Overall, this suggests a higher outdoor air quality co-benefits for shale gas development if it occurs sooner.

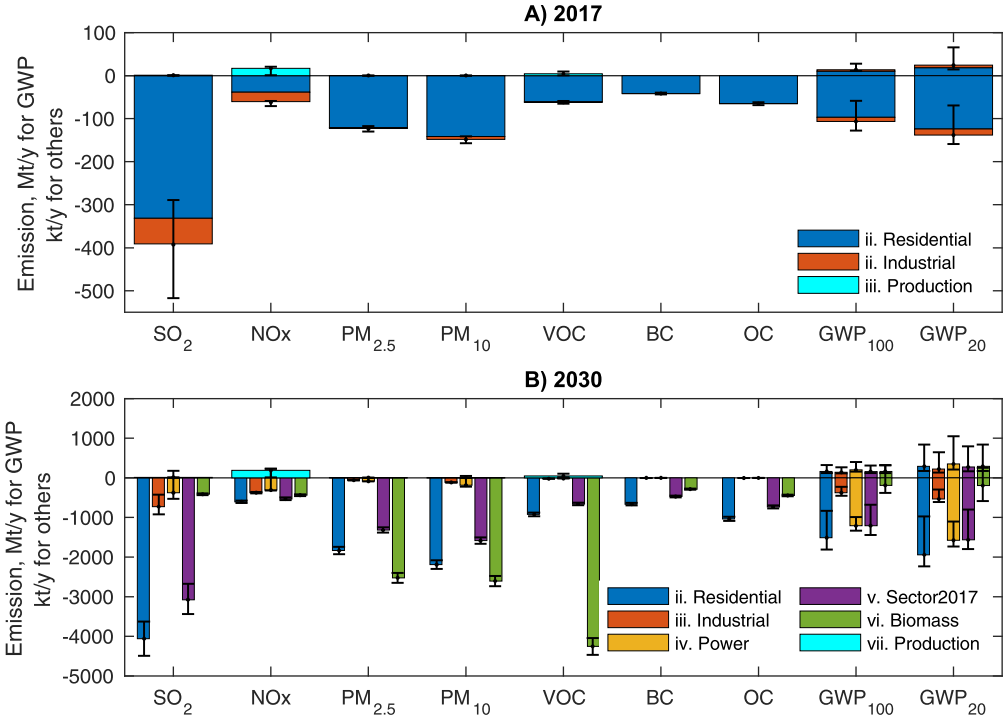

Fig. 2. Changes in air pollutants and GWP associated with shale gas development in 2017 and 2030. Positive emissions are resulted from the upstream processes of shale gas, while negative ones are owing to substituting fuels by shale gas. For 2030, results for five scenarios are shown. No data for BC and OC emissions is available from the upstream processes of shale gas. Vertical lines show the range of uncertainties associated with the variability of emission factors.

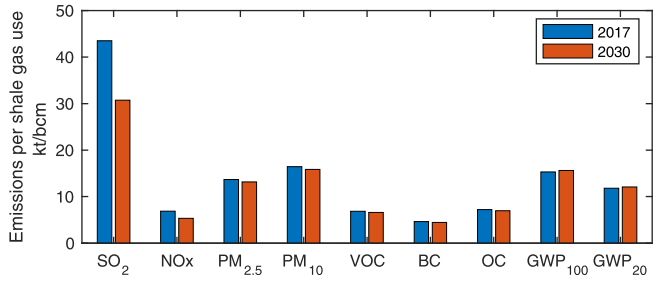

Fig. 3. Air pollutants and GWP emission reductions per unit shale gas replacement for coal combustion in 2017 and 2030 (scenario Sector2017).

3.2. Changes in outdoor $PM_{2.5}$ concentrations

We use the GEOS-Chem model to simulate the outdoor $\Delta PM_{2.5}$ concentrations caused by shale gas development. Overall, the model has no significant bias with simulated base case concentrations (49.0 ± 28.4 μg m^{-3}, the Base scenario in 2017) against observed concentrations in Chinese cities in 2015 (49.9 ± 18.2 μg m^{-3}) ($n = 375$, $r^2 = 0.47$) (list of city names and data are provided in the supporting information) (MEEC, 2018). The discrepancy becomes larger for individual sites or grids (Fig. 4). Nevertheless, the uncertainty is considered smaller as the deviations may be partially canceled when calculating the difference between scenarios.

Fig. 5A shows the decrease of annual mean $PM_{2.5}$ concentration as a result of shale gas substitution ($\Delta PM_{2.5}|_{sub}$) in 2017. The national average $\Delta PM_{2.5}|_{sub}$ is 0.28 μg m^{-3} with a spatial pattern similar to that of shale gas consumption. The highest $\Delta PM_{2.5}|_{sub}$ concentrations are simulated over eastern Sichuan (4 μg m^{-3}) and Henan province (3 μg m^{-3}). The $\Delta PM_{2.5}|_{sub}$ are also elevated over Hubei and Hunan provinces (1–2 μg m^{-3}), as well as Yunnan and Guizhou provinces (1 μg m^{-3}). The $\Delta PM_{2.5}|_{sub}$ in other provinces are generally small: 0.5 μg m^{-3} in East China and almost zero in Northwest and Northeast China. Compared with the base case (i.e. without shale gas substitution), the national average $\Delta PM_{2.5}|_{sub}$ takes account for only 0.78%, but with higher fractions over high shale gas consumption areas such as Sichuan (4.2%) and Henan (3.2%) provinces.

Depending on the assumptions about the sectors and fuel types for shale gas substitution, the predicted national average $\Delta PM_{2.5}|_{sub}$ in 2030 are 0.10 μg m^{-3} (accounting for 0.37% of base case in 2030), 0.14 μg m^{-3} (0.54%), 4.2 μg m^{-3} (15%), and 1.0 μg m^{-3} (3.6%) for the Power, Industrial, Residential, and Biomass scenarios, respectively (Fig. 5B-E). Assuming the sector allocation in 2030 keeps the same as that in 2017 (the Sector2017 scenario) results in an average $\Delta PM_{2.5}|_{sub}$ of 2.9 μg m^{-3} (11%, Fig. 5B). The regions with high $\Delta PM_{2.5}|_{sub}$ shift to the North China Plain (NCP) and Yangtze River Delta (YRD). The highest grid-level $\Delta PM_{2.5}|_{sub}$ is -34.7 μg m^{-3} (57%). The provincial average of $\Delta PM_{2.5}|_{sub}$ are the highest over Shanghai (15.4 μg m^{-3}, 34.4%), Tianjin (16.8 μg m^{-3}, 18.5%), and Beijing (14.4 μg m^{-3}, 20.2%), followed by Henan (13.4 μg m^{-3}, 14.4%), Jiangsu (12.6 μg m^{-3}, 21.9%), Shandong (11.9 μg m^{-3}, 16.3%), and Hebei (10.3 μg m^{-3}, 15.3%) provinces in the NCP and YRD regions. Other provinces in East China have smaller $\Delta PM_{2.5}|_{sub}$ (< 10 μg m^{-3}), accounting for 10–15% of the base case. The provinces in western China such as Xinjiang and Tibet have the smallest $\Delta PM_{2.5}|_{sub}$ (< 1 μg m^{-3}).

The increases of $PM_{2.5}$ concentrations by the upstream processes ($\Delta PM_{2.5}|_{up}$, Fig. 6) are concentrated at production regions located in Southwest China (near the border of Sichuan with Chongqing, Yunnan, and Guizhou provinces). The national average $\Delta PM_{2.5}|_{up}$ is 0.0080 μg m^{-3} and 0.088 μg m^{-3} in 2017 and 2030, respectively. These are much smaller than $\Delta PM_{2.5}|_{sub}$: accounting for 2.8% of the $\Delta PM_{2.5}|_{sub}$ in 2017, and 3.0% in 2030 (Sector2017 scenario). However, the percentages could be much larger for other scenarios in 2030 (e.g. 87% and 61% for Power and Industrial scenarios, respectively). If only considering Sichuan province, the $\Delta PM_{2.5}|_{up}$ are 0.095 and 1.0 μg m^{-3} in 2017 and 2030, respectively, accounting for 8.5% and 34% (Sector2017 scenario) of the $\Delta PM_{2.5}|_{sub}$ for the corresponding years. Interestingly, we find that the $\Delta PM_{2.5}|_{up}$ of Sichuan (1.0 μg m^{-3}), which is the main production region, outweighs the $\Delta PM_{2.5}|_{sub}$ under the Power (0.27 μg m^{-3}) and Industrial (0.29 μg m^{-3}) scenarios in 2030. This indicates an air quality penalty for this province if deploying shale gas in the industrial and power sectors. Similar penalty effects are also predicted for other production provinces such as Chongqing, Yunnan, and Guizhou if deploying shale gas in the power sector in 2030.

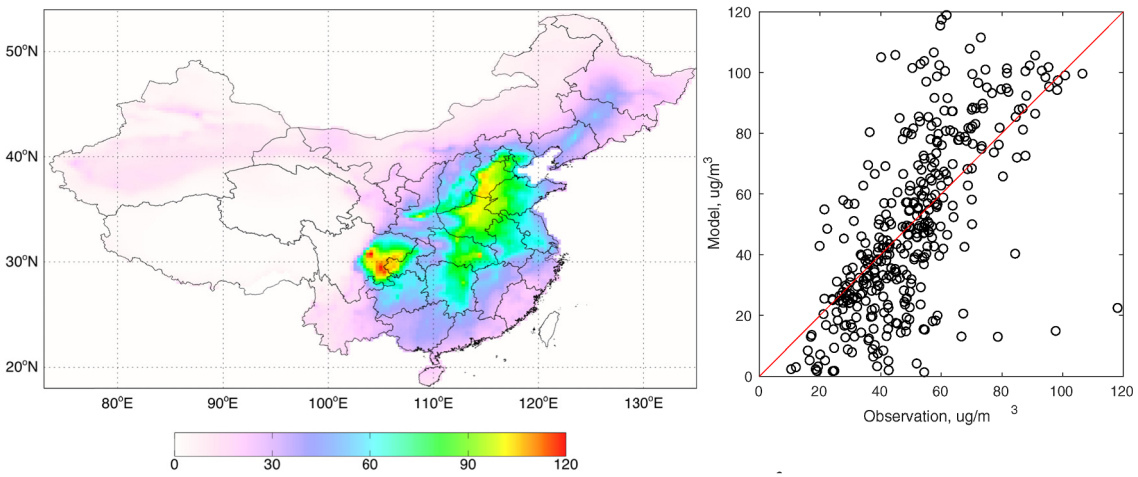

Fig. 4. Base case annual average $PM_{2.5}$ concentrations (μg m^{-3}) near the ground in 2017 simulated by the GEOS-Chem model (left) and a comparison of modeled and observed $PM_{2.5}$ concentrations over 375 Chinese cities in 2015 (right).

3.3. Health impact

Table 2 shows the provincial total avoided premature deaths associated with shale gas substitution (ΔM_{sub}) in 2017. The national total ΔM_{sub} is 27,400 (CI95: 22,870–32,270) with 14,000 (10,650–17,160) and 13,400 (10,350–17,100) for outdoor and indoor air quality, respectively. These avoided premature deaths are mainly from stroke and IHD (48.4%), following by COPD (29.2%) and LC (22.4%). Henan and Sichuan provinces have the largest avoided deaths, 4900 and 4800, respectively, followed by Hunan and Hubei (2,800) provinces. Other provinces have < 2000 avoided deaths.

Similar to emissions and $\Delta PM_{2.5}$ concentrations, the projected ΔM_{sub} varies drastically among shale gas consumption scenarios in 2030 (Table 2). The Residential scenario has the largest ΔM_{sub}, 262,550 (199,670–321,750) and 200,610 (155,310–256,450) for outdoor and indoor air quality, respectively. The avoided premature death from outdoor air pollution for this scenario is 34 and 48 times higher than the Industrial and Power sectors, respectively (Table 2). The benefits from indoor air quality for Residential scenario even stand out as the Industrial and Power sectors have zero benefits in terms of indoor air quality. The Biomass scenario has smaller but still substantial avoided deaths of 64,000 (48,670–78,430) from outdoor air quality. The benefits of indoor air quality are the same for the Residential and Biomass scenarios, as current epidemiological data for the health impact of indoor air pollution cannot differentiate the types of solid fuels (World Health Organization, 2019). Assuming the sector allocation of shale gas consumption in 2030 keeps the same as that in 2017 (i.e. the Sector2017 scenario) results in avoided deaths of 185,580 (14,130–22,770) and 148,450 (11,490–18,980) for outdoor and indoor air quality, respectively. The provincial distribution of ΔM_{sub} is significantly different from that in 2017, with the highest ΔM_{sub} from Jiangsu (29,700), Shandong (29,600), Henan (26,900), Guangdong (26,500), Hebei (21,100), Anhui (16,400), and Sichuan (14,400) provinces.

The national total excess premature deaths attributable to upstream processes (ΔM_{up}) in 2017 are estimated to be 347 (264–425) with Sichuan (2 1 2), Chongqing (55), Guizhou (27) and Yunnan (22) contributing 91% of the national total. This calculated ΔM_{up} accounts for only 1.3% of the national total ΔM_{sub}. In 2030, the predicted ΔM_{up} amount to 3850 (2930–4720) with similar provincial distribution as 2017 (Table 2). We find the predicted ΔM_{up} can exceed the ΔM_{sub} in some provinces in 2030. For example, the ΔM_{up} is projected to be 2350 in Sichuan province, which is larger than the ΔM_{sub} of this province for the Power (800) and Industrial (860) scenarios. A similar situation happens to Chongqing, Yunnan and Guizhou provinces. This indicates a potential net local increase in mortality in these regions due to upstream emissions if deploying shale gas in the power and industrial sectors, despite a net decrease in the national total premature mortality.

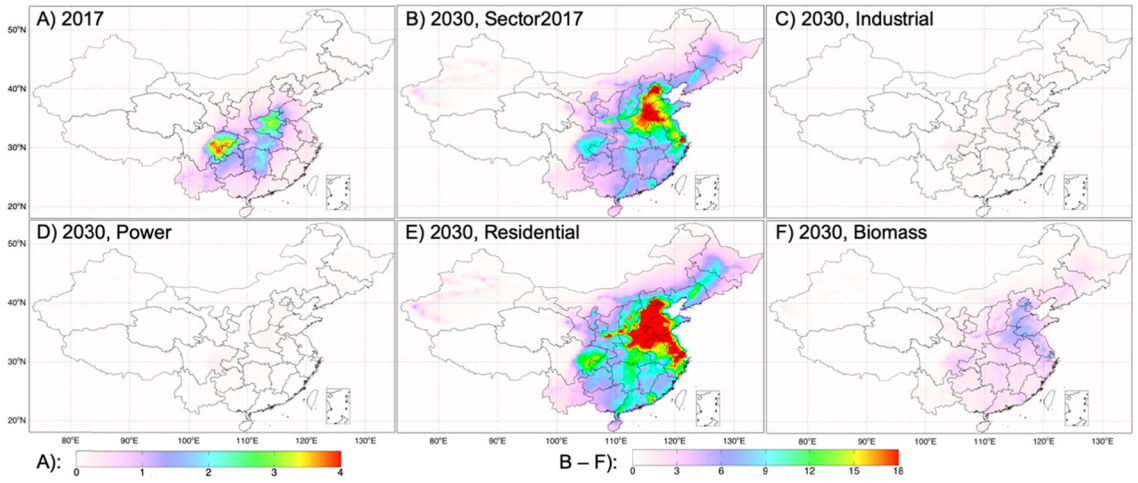

Fig. 5. Decreases in annual mean $PM_{2.5}$ concentrations (μg m^{-3}) resulted from substituting other fuels with shale gas in 2017 (A) and 2030 (B-F). Panels B-F are for Sector2017, Industrial, Power, Residential, and Biomass scenarios, respectively (Table 1). Note the different color bars for panel A and panel B-F.

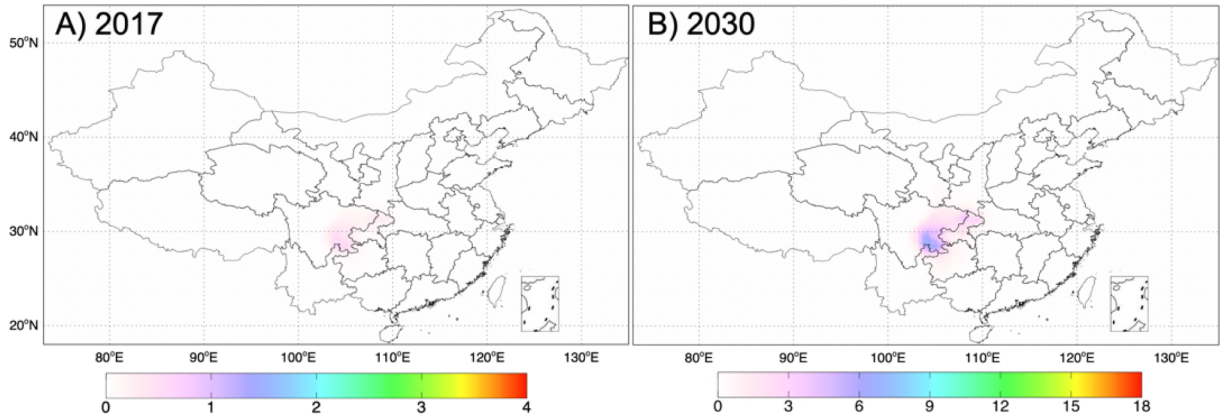

Fig. 6. Projected increases of annual mean $PM_{2.5}$ concentrations (μg m^{-3}) caused by the upstream processes in (A) 2017 and (B) 2030.

3.4. Uncertainties

The results presented here have several limitations and subject to uncertainties. The actual total emissions and emission factors are likely different from the prediction from the GAINS model. Due to the computational cost, we run the GEOS-Chem model with only the best estimate emissions, as the majority of the overall uncertainty of health impact is derived from that of exposure-effect relationships (Qin et al., 2017; Wang et al., 2017). We use population data or total primary energy needs as proxies to distribute the shale gas consumption data to individual provinces and model grids. This bears uncertainties as the actual consumption is influenced by factors such as proximity to production regions, pipeline infrastructures, and availability of other energy sources (Yue and Long, 2013). The estimate of indoor air quality

Table 2
Avoided (or excess) premature death of each province in mainland China associated with outdoor (Out) and indoor (In) air pollution caused by shale gas upstream processes and fuel substitution in 2017 and 2030.

Province	2017			2030									
	Substitution		Upstream	Substitution									Upstream
				Sector 2017		Industrial		Residential		Power		Biomass	
	Out	In		Out	In	Out	In	Out	In	Out	In	Out	In	
Anhui	567	233	0	10,820	5659	319	0	15,374	7648	180	0	3731	7648	3
Beijing	55	9	0	4020	2440	134	0	5710	3298	144	0	1386	3298	0
Chongqing	832	779	55	3148	2050	200	0	4413	2771	201	0	1086	2771	607
Fujian	155	81	0	5237	3679	102	0	7481	4971	57	0	1806	4971	4
Gansu	104	21	4	2158	2840	112	0	3039	3838	93	0	744	3838	48
Guangdong	454	43	2	14,573	12,049	441	0	20,709	16,282	248	0	5025	16,282	25
Guangxi	387	49	3	4541	3338	244	0	6396	4511	166	0	1566	4511	28
Guizhou	561	1229	27	3430	3054	246	0	4793	4127	225	0	1183	4127	296
Hainan	36	3	0	633	664	29	0	895	898	18	0	218	898	1
Hebei	349	85	0	11,740	9464	504	0	16,578	12,789	342	0	4048	12,789	3
Heilongjiang	32	36	0	3517	3864	277	0	4906	5222	174	0	1213	5222	0
Henan	2171	2783	4	16,914	10,076	886	0	23,812	13,616	637	0	5832	13,616	43
Hong Kong	4	0	0	26	0	1	0	37	0	1	0	9	0	0
Hubei	1002	1843	6	6844	4666	304	0	9681	6305	190	0	2360	6305	67
Hunan	1293	1502	2	7375	4105	346	0	10,417	5547	215	0	2543	5547	23
Inner Mogolia	31	47	0	2594	5964	135	0	3655	8060	86	0	894	8060	2
Jiangsu	525	253	0	18,327	11,395	374	0	26,161	15,399	192	0	6320	15,399	4
Jiangxi	262	106	0	4591	3112	117	0	6540	4206	67	0	1583	4206	2
Jilin	29	29	0	2940	3163	210	0	4111	4274	139	0	1014	4274	0
Liaoning	80	50	0	6018	6461	336	0	8467	8731	201	0	2075	8731	2
Maco	3	0	0	88	0	3	0	125	0	2	0	30	0	0
Ningxia	18	8	1	640	1677	22	0	908	2267	19	0	221	2267	7
Qinghai	5	6	0	351	582	14	0	496	786	19	0	121	786	1
Shaanxi	277	34	6	4727	3890	191	0	6689	5257	131	0	1630	5257	69
Shandong	784	466	1	17,437	12,289	653	0	24,703	16,606	431	0	6013	16,606	7
Shanghang	122	46	0	5007	4917	62	0	7176	6645	33	0	1727	6645	1
Shanxi	212	63	1	5475	6793	194	0	7772	9179	136	0	1888	9179	11
Sichuan	2555	2282	212	9089	5359	861	0	12,582	7242	804	0	3134	7242	2347
Tianjin	5	12	0	301	2157	10	0	427	2914	7	0	104	2914	0
Tibet	2	1	0	9	98	1	0	12	133	0	0	3	133	0
Xinjiang	11	22	0	675	1973	27	0	956	2666	27	0	233	2666	0
Yunnan	745	1082	22	2901	2792	208	0	4056	3774	182	0	1000	3774	248
Zhejiang	307	118	0	9433	7877	162	0	13,470	10,645	67	0	3253	10,645	2
Total	13,972	13,374	347	185,579	148,448	7725	0	262,549	200,606	5433	0	63,993	200,606	3851

health impact is also subjected to large uncertainties due to assumptions such as household type, family size, shale gas consumption pattern.

Our study does not consider the interaction of shale gas with other natural gas sources and renewable energy (e.g. wind and solar), which may have a competing effect in replacing coal and biomass fuels. Our results thus should be considered as diagnostic and a dynamic supply-demand model for multiple energy sources is required for a more accurate projection (Ma and Li, 2010). Also, the projected shale gas production may substantially modify the energy structure in some sectors. The projected shale gas consumption in the residential sector amounts to 74 bcm in 2030 (Sector2017 scenario). This is close to the natural gas (82 bcm) required to replace all the coal use in the residential and commercial sectors (2.1×10^8 tons) (NBSC, 2016). The shale gas will be highly likely to replaces coal and biomass fuels simultaneously in the residential sector. The replaced agricultural waste used as biomass fuels may be directly burned in the field, which could cause air pollution and compromises the benefits of shale gas substitution (Chen et al., 2016). Our estimate for the health benefits associated with indoor air quality in 2030 also subjects to uncertainty as the population relying on solid fuel (P_{SF}) and the related death ($M_{baseline}$) are both continuous decreasing (Tao et al., 2018). Although these trends may cancel with each other, its net impact on the calculated ΔM is unclear (Eq. (7)).

The emission factors of air pollutants during production depend on local geologic factors (e.g. pad condition and drilling depth) and the fracturing fleet conditions, whereas the upstream fugitive CH_4 emission factor largely depends on the flaring ratio. The reported emission factors for the upstream processes of shale gas production in China are very scarce and subject to large uncertainties. These emission factors may be substantially reduced if regulations are enforced by the government. We use air pollutant emission factors collected from the literature and assume the flaring ratio to be the same as that in the U.S. before its methane regulation in 2012 (Qin et al., 2017; Chang et al., 2014). Indeed, more on-site emission measurements, especially for NOx, VOC, and CH_4 are needed.

The projections for future shale gas productions in China bear large variabilities among organizations and subject to frequent adjustment (Fig. 7). In recent years, fast technical advancement has been achieved by Chinese oil companies (HBERC, 2018); and the average cost for gas wells has decreased by 20–40% since 2014 (Wood Mackenzie, 2019a). A recent well is reported to have a daily production of 1.4 mcm, equivalent to ~1/20 of current annual production (Yang et al., 2019). On the other hand, more than half of the reserves in the southern Sichuan region are buried > 3500 m down in structures warped by active faultlines, which increases the technical difficulties for exploitation (NEAC, 2020). The lack of an open and competitive exploitation market also affects the pace of shale gas development (Tian et al., 2014). As a result, the NEAC had lowered the production target for 2020 (60–100 bcm) made in 2012 to 30 bcm in 2016 (NEAC, 2020; NDRC, 2020). It was recently projected that the production amounts to 15 bcm in 2020, and the 2020 goal is delayed to 2024 (HBERC, 2018). The 2040 goal is also reduced from 132 bcm to 88 bcm (Wood Mackenzie, 2019a, 2019b). The lag in fulfilling previously made targets indicates a possible delay in achieving the government plan of 2030.

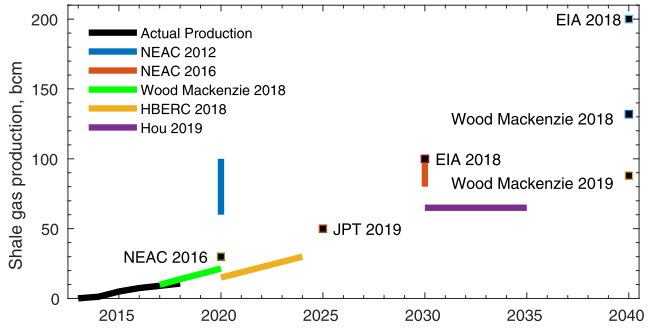

Fig. 7. Production of Shale gas in China during 2013–2018 and projections to 2040 (NEAC, 2019, 2020; NDRC, 2020; HBERC, 2018; Hou, 2019; Journal of Petroleum Technology, 2019; Wood Mackenzie, 2019a, 2019b).

3.5. Policy implications

By assuming no reduction in emission factors during shale gas production in 2030, our analysis indicates that the deteriorating of local air quality may outweigh its benefits at a regional scale under certain deploying scenarios. Similar regional offsets and trade-offs are also found for ozone air quality in Texas, U.S. as a result of the development of Eagle Ford Shale (Pacsi et al., 2015). The potential severe local air quality impact, together with other environmental risk factors such as water pollution and earthquakes, might influence the further development of shale gas by local governments in China (Sichuan Government, 2019). This highlights the importance of more stringent emission control (including major air pollutants and methane leakage) during shale gas production processes. Emission standards and regulations, similar to the revised Oil and Gas Rule by the US EPA, are also needed in China (US EPA, 2019).

We find that the health benefit of shale gas development associated with indoor air quality is close to that of outdoor air quality in 2017. In 2030, we find interesting alignments and trade-offs among different scenarios about outdoor air quality, indoor air quality, and GWP emissions. The Residential scenario has the largest outdoor and indoor air quality benefits and GWP emission reductions, but it may be challenged by the distribution infrastructure and deployment cost. The Biomass scenario is similar to the Residential one, but it causes a close to neutral impact on GWP emissions. The Industrial and Power scenarios have the least outdoor air quality and zero indoor air quality benefits, but they still have a substantial GWP emission reduction (especially the Power scenario).

In conclusion, we suggest a priority in deploying shale gas in place of coal in the residential sectors due to co-benefit in outdoor and indoor air quality. However, we consider our results illustrative and leave it to the central and local governments to balance the costs and benefits in all aspects, especially regarding the required cost associated with pipeline construction and/or liquified natural gas distribution. Significant regional variability and offsets are also noted, including the net penalty effect projected for some scenarios in shale gas production regions. This calls for more stringent emission control during upstream processes, and also requires a comprehensive consideration of the cost and benefits of the shale gas industry in the airshed and even the whole country.

CRediT authorship contribution statement

Yanxu Zhang: Conceptualization, Methodology, Data curation, Investigation, Visualization, Supervision, Project administration, Funding acquisition, Writing - original draft. **Haikun Wang:** Conceptualization, Methodology, Data curation, Investigation, Writing - review & editing. **Yun Han:** Methodology, Data curation, Investigation. **Danhan Wang:** Methodology, Data curation, Investigation. **Ge Zhu:** Methodology, Data curation, Investigation. **Xi Lu:** Conceptualization, Methodology, Writing - review & editing.

Declaration of Competing Interest

The authors declare that they have no known competing financial interests or personal relationships that could have appeared to influence the work reported in this paper.

Acknowledgment

This study was supported by the National Key R&D Program of China (2019YFA0606803), Start-up fund of the Thousand Youth Talents Plan, Jiangsu Innovative and Entrepreneurial Talents Plan, and the Collaborative Innovation Center of Climate Change, Jiangsu Province. We thank Minghuai Wang to provides help in obtaining the shale gas survey data; Guofeng Shen and Xi Zhu to provide site $PM_{2.5}$ data; Jintai Lin, Hancheng Dai, and Wei Du for helpful discussions.

Appendix A. Supplementary material

Supplementary data to this article can be found online at https://doi.org/10.1016/j.envint.2020.105727.

References

Amann, M., Bertok, I., Borken-Kleefeld, J., Chambers, A., Cofala, J., Dentener, F., Heyes, C., Höglund-Isaksson, L., Klimont, Z., Purohit, P., et al., 2008. GAINS Asia. A tool to combat air pollution and climate change simultaneously. Methodology.

Amann, M., Kejun, J., Jiming, H.A.O., Wang, S., Xing, Z., Xiang, D.Y., Hong, L., Jia, X., Chuying, Z., Bertok, I., et al., 2008. GAINS Asia. Scenarios for Cost-Effective Control of Air Pollution and Greenhouse Gases in China.

Burnett, R.T., Arden Pope, C., Ezzati, M., Olives, C., Lim, S.S., Mehta, S., Shin, H.H., Singh, G., Hubbell, B., Brauer, M., et al., 2014. An Integrated risk function for estimating the global burden of disease attributable to ambient fine particulate matter exposure. Environ. Health Perspect. 122 (4), 397–403. https://doi.org/10.1289/ehp.1307049.

Center for Earth System Science of Tsinghua University, 2019. Multi-resolution emission inventory of China. http://www.meicmodel.org (accessed Dec 9, 2019).

Chang, Y., Huang, R., Ries, R.J., Masanet, E., 2014. Shale-to-well energy use and air pollutant emissions of shale gas production in China. Appl. Energy 125, 147–157. https://doi.org/10.1016/j.apenergy.2014.03.039.

Chen, J., Li, C., Ristovski, Z., Milic, A., Gu, Y., Islam, M.S., Wang, S., Hao, J., Zhang, H., He, C., et al., 2016. A review of biomass burning: emissions and impacts on air quality, health and climate in China. Sci. Total Environ. 2017 (579), 1000–1034. https://doi.org/10.1016/j.scitotenv.2016.11.025.

Chen, Y., Zhi, G., Feng, Y., Liu, D., Zhang, G., Li, J., Sheng, G., Fu, J., 2009. Measurements of black and organic carbon emission factors for household coal combustion in China: implication for emission reduction. Environ. Sci. Technol. 43 (24), 9495–9500. https://doi.org/10.1021/es9021766.

de Gouw, J.A., Parrish, D.D., Frost, G.J., Trainer, M., 2014. Reduced emissions of CO2, NOx, and SO2 from U.S. Power plants owing to switch from coal to natural gas. Earth's Futur. 75–82. https://doi.org/10.1002/2013EF000196.Abstract.

Dean Hosgood, H., Boffetta, P., Greenland, S., Lee, Y.C.A., Mclaughlin, J., Seow, A., Duell, E.J., Andrew, A.S., Zaridze, D., Szeszenia-Dabrowska, N., et al., 2010. In-home coal and wood use and lung cancer risk: a pooled analysis of the international lung cancer consortium. Environ. Health Perspect. https://doi.org/10.1289/ehp.1002217.

Du, W., Li, X., Chen, Y., Shen, G., 2018. Household air pollution and personal exposure to air pollutants in rural China – a review. Environ. Pollut. 237, 625–638. https://doi.org/10.1016/j.envpol.2018.02.054.

Fisher, J.A., Jacob, D.J., Travis, K.R., Kim, P.S., Marais, E.A., Miller, C.C., Yu, K., Zhu, L., Yantosca, R.M., Sulprizio, M.P., et al., 2016. Organic nitrate chemistry and its implications for nitrogen budgets in an isoprene- and monoterpene-rich atmosphere: constraints from aircraft (SEAC4RS) and ground-based (SOAS) observations in the Southeast US. Atmos. Chem. Phys. https://doi.org/10.5194/acp-16-5969-2016.

Guenther, A.B., Jiang, X., Heald, C.L., Sakulyanontvittaya, T., Duhl, T., Emmons, L.K., Wang, X., 2012. The model of emissions of gases and aerosols from nature version 2.1 (MEGAN2. 1): an extended and updated framework for modeling biogenic emissions. Geosci. Model Dev. https://doi.org/10.5194/gmd-5-1471-2012.

Guo, M., Lu, X., Nielsen, C.P., McElroy, M.B., Shi, W., Chen, Y., Xu, Y., 2016. Prospects for shale gas production in china: implications for water demand. Renew. Sustain. Energy Rev. 66, 742–750. https://doi.org/10.1016/j.rser.2016.08.026.

HBERC, 2018. China Shale Gas Market Survey Report and Developing Outlook (2018–2024); 2018.

Hou, R., 2019. Chinese shale gas production may hit 65 bcm per year. https://www.jiemian.com/article/3460983.html (accessed Aug 31, 2019).

Howarth, R.W., Ingraffea, A., Engelder, T., 2011. Should fracking stop? Nature 477, 271–275.

IIASA, 2019. The Greenhouse Gas – Air Pollution Interactions and Synergies (GAINS) model http://www.iiasa.ac.at/web/home/research/researchPrograms/air/Asia.html (accessed Jul 1, 2019).

Jiang, Kai, Ashworth, Peta, Zhang, Shiyi, Liang, Xi, Sun, Yan, Angus, Daniel, 2020. China's carbon capture, utilization and storage (CCUS) policy: a critical review. Renew. Sustain. Energy Rev. 119, 109601. https://doi.org/10.1016/j.rser.2019.109601.

Journal of Petroleum Technology, 2019. China Shale Gas: CNPC Seeks To Double Sichuan Output By 2025. https://pubs.spe.org/en/jpt/jpt-article-detail/?art=5816 (accessed Aug 9, 2019).

Krupnick, A., Wang, Z., Wang, Y., 2014. Environmental risks of shale gas development in China. Energy Policy 75, 117–125. https://doi.org/10.1016/j.enpol.2014.07.022.

Liu, J., Mauzerall, D.L., Chen, Q., Zhang, Q., Song, Y., Peng, W., Klimont, Z., Qiu, X., Zhang, S., Hu, M., et al., 2016. Air pollutant emissions from chinese households: a major and underappreciated ambient pollution source. Proc. Natl. Acad. Sci. U.S.A. 113 (28), 7756–7761. https://doi.org/10.1073/pnas.1604537113.

Ma, Y., Li, Y., 2010. Analysis of the supply-demand status of china's natural gas to 2020. Pet. Sci. 7 (1), 132–135. https://doi.org/10.1007/s12182-010-0017-9.

Mao, X., Guo, X., Chang, Y., Peng, Y., 2005. Improving air quality in large cities by substituting natural gas for coal in China: changing idea and incentive policy implications. Energy Policy. https://doi.org/10.1016/j.enpol.2003.08.002.

Matus, K., Nam, K.M., Selin, N.E., Lamsal, L.N., Reilly, J.M., Paltsev, S., 2012. Health damages from air pollution in China. Glob. Environ. Chang. 22 (1), 55–66. https://doi.org/10.1016/j.gloenvcha.2011.08.006.

MEEC, 2018. Historical air quality data for cities http://beijingair.sinaapp.com (accessed Jan 1, 2018).

Myhre, G., Shindell, D., Bréon, F.-M., Collins, W. D., Fuglestvedt, J., Huang, J., Koch, D., Lamarque, J.-F., Lee, D., Mendoza, B., et al., 2013. IPCC AR5 (2013) Chapter 8: Anthropogenic and Natural Radiative Forcing. In: Climate Change 2013: The Physical Science Basis. Contribution of Working Group I to the Fifth Assessment Report of the Intergovernmental Panel on Climate Change; 2013. https://doi.org/10.1017/CBO9781107415324.018.

Miller, C., Jacob, D.J., Marais, E.A., Yu, K., Travis, K.R., Kim, P.S., Fisher, J.A., Zhu, L., Wolfe, G.M., Hanisco, T.F., et al., 2017. Glyoxal yield from isoprene oxidation and relation to formaldehyde: chemical mechanism, constraints from SENEX aircraft observations, and interpretation of OMI satellite data. Atmos. Chem. Phys. https://doi.org/10.5194/acp-17-8725-2017.

NBSC, 2016. China Energy Statistical Yearbook 2016. China Statistics Press, Beijing.

NDRC, 2019. Mid- and long-term oil and natural gas pipeline network plan. http://www.ndrc.gov.cn/zcfb/zcfbghwb/201707/W020170712525204531251.pdf (accessed Aug 26, 2019).

NDRC, 2020. Shale gas development plan (2011–2015). http://www.ndrc.gov.cn/zcfb/zcfbtz/201203/t20120316_467518.html (accessed Apr 27, 2020).

NEAC, 2019. Shale gas industry policy. http://www.ndrc.gov.cn/zcfb/zcfbtz/201203/t20120316_467518.html (accessed Aug 8, 2019).

NEAC, 2020. Shale gas development plan (2016–2020). http://www.gov.cn/xinwen/2016-09/30/content_5114313.htm (accessed Apr 27, 2020).

Pacsi, A.P., Kimura, Y., McGaughey, G., McDonald-Buller, E.C., Allen, D.T., 2015. Regional ozone impacts of increased natural gas use in the Texas power sector and development in the eagle ford shale. Environ. Sci. Technol. 49 (6), 3966–3973. https://doi.org/10.1021/es5055012.

Qin, Y., Wagner, F., Scovronick, N., Peng, W., Yang, J., Zhu, T., Smith, K.R., Mauzerall, D.L., 2017. Air quality, health, and climate implications of China's synthetic natural gas development. Proc. Natl. Acad. Sci. U.S.A. 114 (19), 4887–4892. https://doi.org/10.1073/pnas.1703167114.

Qin, Y., Edwards, R., Tong, F., Mauzerall, D.L., 2017. Can switching from coal to shale gas bring net carbon reductions to China? Environ. Sci. Technol. 51 (5), 2554–2562. https://doi.org/10.1021/acs.est.6b04072.

Qin, Y., Höglund-Isaksson, L., Byers, E., Feng, K., Wagner, F., Peng, W., Mauzerall, D.L., 2018. Air quality–carbon–water synergies and trade-offs in China's Natural Gas Industry. Nat. Sustain. 1 (9), 505–511. https://doi.org/10.1038/s41893-018-0136-7.

Randerson, J.T., van der Werf, G.R., Giglio, L., Collatz, G.J., Kasibhatla, P.S., 2018. Global Fire Emissions Database. ORNL DAAC, Oak Ridge, Tennessee, USA. Version 4.1, (GFEDv4). https://doi.org/10.3334/ORNLDAAC/1293.

Shen, G., Ru, M., Du, W., Zhu, X., Zhong, Q., Chen, Y., Shen, H., Yun, X., Meng, W., Liu, J., et al., 2019. Impacts of air pollutants from rural chinese households under the rapid residential energy transition. Nat. Commun. 10 (1), 1–8. https://doi.org/10.1038/s41467-019-11453-w.

Sichuan Government, 2019. Rong County stops shale gas development since February 26, 2019. http://www.sc.gov.cn/10462/12771/2019/2/25/c172a163dc804118962c608f93dba76e.shtml (accessed Mar 12, 2019).

Song, W., Chang, Y., Liu, X., Li, K., Gong, Y., He, G., Wang, X., Christie, P., Zheng, M., Dore, A.J., et al., 2015. A multiyear assessment of air quality benefits from China's emerging shale gas revolution: urumqi as a case study. Environ. Sci. Technol. 49 (4), 2066–2072. https://doi.org/10.1021/es5050024.

Stanaway, J.D., Afshin, A., Gakidou, E., Lim, S.S., Abate, D., Abate, K.H., Abbafati, C., Abbasi, N., Abbastabar, H., Abd-Allah, F., et al., 2018. Global, regional, and national comparative risk assessment of 84 behavioural, environmental and occupational, and metabolic risks or clusters of risks for 195 countries and territories, 1990–2017: a systematic analysis for the global burden of disease Stu. Lancet. https://doi.org/10.1016/S0140-6736(18)32225-6.

Tao, S., Ru, M.Y., Du, W., Zhu, X., Zhong, Q.R., Li, B.G., Shen, G.F., Pan, X.L., Meng, W.J., Chen, Y.L., et al., 2018. Quantifying the Rural Residential Energy a Representative National Survey. https://doi.org/10.1038/s41560-018-0158-4.

Tian, L., Wang, Z., Krupnick, A., Liu, X., 2014. Stimulating shale gas development in China: a comparison with the US experience. Energy Policy 75, 109–116. https://doi.org/10.1016/j.enpol.2014.07.025.

US EIA, 2019. Shale Gas Production. https://www.eia.gov/dnav/ng/ng_prod_shalegas_s1_a.htm (accessed Mar 10, 2019).

US EIA, 2019. World Shale Resource Assessments. https://www.eia.gov/analysis/studies/worldshalegas/ (accessed Mar 10, 2019).

US EPA, 2019. Controlling Air Pollution from the Oil and Natural Gas Industry. https://www.epa.gov/controlling-air-pollution-oil-and-natural-gas-industry/new-source-performance-standards-and (accessed Dec 9, 2019).

US EIA, 2020. China adds incentives for domestic natural gas production as imports increase. https://www.eia.gov/todayinenergy/detail.php?id=41773 (accessed Jan 15, 2020).

Wang, H., Zhang, Y.Y., Zhao, H., Lu, X., Zhang, Y.Y., Zhu, W., Nielsen, C.P., Li, X., Zhang, Q., Bi, J., et al., 2017. Trade-driven relocation of air pollution and health impacts in China. Nat. Commun. https://doi.org/10.1038/s41467-017-00918-5.

Wood Mackenzie, 2019a. Chinese shale gas production will almost double in two years. https://www.woodmac.com/news/editorial/chinese-shale-gas-production-will-almost-double-in-two-years (accessed Aug 28, 2019).

Wood Mackenzie, 2019b. China's gas production to double to 325 bcm in 2040. https://www.woodmac.com/press-releases/chinas-gas-production-to-double-to-325-bcm-in-2040 (accessed Aug 28, 2019).

World Health Organization, 2019. Burden of disease from household air pollution for 2016: Description of method. https://www.who.int/airpollution/data/HAP_BoD_methods_May2018.pdf?ua=1 (accessed Aug 30, 2019).

Yu, K., Qiu, G., Chan, K.H., Lam, K.B.H., Kurmi, O.P., Bennett, D.A., Yu, C., Pan, A., Lv, J., Guo, Y., et al., 2018. Association of solid fuel use with risk of cardiovascular and all-cause mortality in rural China. JAMA – J. Am. Med. Assoc. 319 (13), 1351–1361. https://doi.org/10.1001/jama.2018.2151.

Yue, T., Long, R., 2013. Analysis of influencing factors of China's household energy consumption. East China Econ. Manag. 27 (11), 57–61.

Yang, H., Zhao, X., Feng, X., Huang, Y., Xiong, X., Yin, Z., Xiao, Y., 2019. The first shale gas well with daily production more than a million cubic meters in China. https://www.sohu.com/a/299591511_683414 (accessed Mar 12, 2019).

Zhang, L., Henze, D.K., Grell, G.A., Bousserez, N., Zhang, Q., Torres, O., Ahn, C., Lu, Z., Cao, J., Mao, Y., et al., 2015. Constraining Black Carbon Aerosol over Asia Using OMI Aerosol Absorption Optical Depth and the Adjoint of GEOS-Chem.

Zhang, Y., Jacob, D.J., Horowitz, H.M., Chen, L., Amos, H.M., Krabbenhoft, D.P., Slemr, F., St. Louis, V.L., Sunderland, E.M., 2016. Observed decrease in atmospheric mercury explained by global decline in anthropogenic emissions. Proc. Natl. Acad. Sci. U.S.A. 113 (3), 526–531. https://doi.org/10.1073/pnas.1516312113.